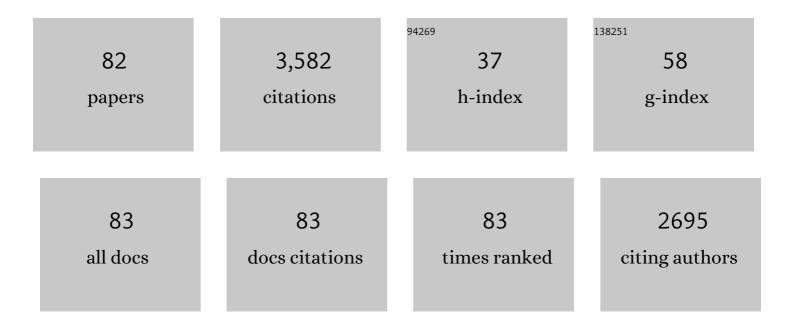
Themiya Nanayakkara

List of Publications by Year in descending order

Source: https://exaly.com/author-pdf/8523694/publications.pdf Version: 2024-02-01



#	Article	IF	CITATIONS
1	Equivalent widths of Lyman <i>α</i> emitters in MUSE-Wide and MUSE-Deep. Astronomy and Astrophysics, 2022, 659, A183.	2.1	16
2	Deciphering stellar metallicities in the early Universe: case study of a young galaxy at <i>z</i> = 4.77 in the MUSE eXtremely Deep Field. Astronomy and Astrophysics, 2022, 660, A10.	2.1	5
3	The ALMA REBELS Survey: cosmic dust temperature evolution out to <i>z</i> â^1⁄4 7. Monthly Notices of the Royal Astronomical Society, 2022, 513, 3122-3135.	1.6	51
4	The MUSE eXtremely Deep Field: Individual detections of Ly <i>α</i> haloes around rest-frame UV-selected galaxies at <i>z</i> â‰f 2.9–4.4. Astronomy and Astrophysics, 2022, 660, A44.	2.1	11
5	EMPRESS. IV. Extremely Metal-poor Galaxies Including Very Low-mass Primordial Systems with M _* = 10 ⁴ –10 ⁵ M _⊙ and 2%–3% (O/H): High (Fe/O) Suggestive of Metal Enrichment by Hypernovae/Pair-instability Supernovae. Astrophysical Journal, 2022, 925, 111.	1.6	16
6	Massive high-redshift quiescent galaxies with JWST. Publications of the Astronomical Society of Australia, 2022, 39, .	1.3	5
7	The ALMA REBELS Survey. Epoch of Reionization giants: Properties of dusty galaxies at <i>z</i> â‰^ 7. Monthly Notices of the Royal Astronomical Society, 2022, 512, 58-72.	1.6	44
8	The Lensed Lyman-Alpha MUSE Arcs Sample (LLAMAS). Astronomy and Astrophysics, 2022, 666, A78.	2.1	15
9	The UV 2175Ã attenuation bump and its correlation with PAH emission at <i>z</i> â^¼ 2. Monthly Notices of the Royal Astronomical Society, 2022, 514, 1886-1894.	1.6	10
10	The MUSE eXtremely deep field: first panoramic view of an Mg†l emitting intragroup medium. Astronomy and Astrophysics, 2022, 663, A11.	2.1	11
11	Reionization Era Bright Emission Line Survey: Selection and Characterization of Luminous Interstellar Medium Reservoirs in the z > 6.5 Universe. Astrophysical Journal, 2022, 931, 160.	1.6	77
12	The ALMA REBELS Survey: dust continuum detections at <i>z</i> > 6.5. Monthly Notices of the Royal Astronomical Society, 2022, 515, 3126-3143.	1.6	46
13	Consistent Dynamical and Stellar Masses with Potential Light IMF in Massive Quiescent Galaxies at 3 < z < 4 Using Velocity Dispersions Measurements with MOSFIRE. Astrophysical Journal Letters, 2021, 908, L35.	3.0	16
14	A low [CII]/[NII] ratio in the center of a massive galaxy at <i>z</i> = 3.7: Evidence for a transition to quiescence at high redshift?. Astronomy and Astrophysics, 2021, 646, A68.	2.1	3
15	An atlas of MUSE observations towards twelve massive lensing clusters. Astronomy and Astrophysics, 2021, 646, A83.	2.1	71
16	The MUSE Extremely Deep Field: The cosmic web in emission at high redshift. Astronomy and Astrophysics, 2021, 647, A107.	2.1	45
17	A low [CII]/[NII] ratio in the center of a massive galaxy at <i>z</i> = 3.7: Evidence for a transition to quiescence at high redshift? <i>(Corrigendum)</i> . Astronomy and Astrophysics, 2021, 650, C2.	2.1	1
18	Measuring the Average Molecular Gas Content of Star-forming Galaxies at z = 3–4. Astrophysical Journal, 2021, 916, 12.	1.6	10

#	Article	IF	CITATIONS
19	New Determinations of the UV Luminosity Functions from z $\hat{a}^{1}/_{4}$ 9 to 2 Show a Remarkable Consistency with Halo Growth and a Constant Star Formation Efficiency. Astronomical Journal, 2021, 162, 47.	1.9	166
20	Recovery and analysis of rest-frame UV emission lines in 2052 galaxies observed with MUSE at 1.5 < <i>z</i> < 6.4. Astronomy and Astrophysics, 2021, 654, A80.	2.1	15
21	Normal, dust-obscured galaxies in the epoch of reionization. Nature, 2021, 597, 489-492.	13.7	71
22	ZFIRE: The Beginning of the End for Massive Galaxies at z â^¼ 2 and Why Environment Matters. Astrophysical Journal, 2021, 919, 57.	1.6	4
23	MOSEL: Strong [Oiii] 5007 Ã Emitting Galaxies at (3 < z < 4) from the ZFOURGE Survey. Astrophysical Journal, 2020, 898, 45.	1.6	16
24	Stellar populations and physical properties of starbursts in the antennae galaxy from self-consistent modelling of MUSE spectra. Monthly Notices of the Royal Astronomical Society, 2020, 497, 3860-3895.	1.6	10
25	Evidence for galaxy quenching in the green valley caused by a lack of a circumgalactic medium. Monthly Notices of the Royal Astronomical Society, 2020, 500, 2289-2301.	1.6	6
26	The nature of CR7 revealed with MUSE: a young starburst powering extended Ly α emission at zÂ= 6.6. Monthly Notices of the Royal Astronomical Society, 2020, 498, 3043-3059.	1.6	11
27	ZFIRE: Measuring Electron Density with [O ii] as a Function of Environment at zÂ=Â1.62. Astrophysical Journal, 2020, 892, 77.	1.6	12
28	Elevated ionizing photon production efficiency in faint high-equivalent-width Lyman-α emitters. Monthly Notices of the Royal Astronomical Society, 2020, 493, 5120-5130.	1.6	45
29	The MUSE <i>Hubble</i> Ultra Deep Field Survey. Astronomy and Astrophysics, 2020, 641, A118.	2.1	28
30	Reconstructing the Observed Ionizing Photon Production Efficiency at z â ⁻¹ ⁄4 2 Using Stellar Population Models. Astrophysical Journal, 2020, 889, 180.	1.6	14
31	MOSEL Survey: Tracking the Growth of Massive Galaxies at 2Â<ÂzÂ<Â4 Using Kinematics and the IllustrisTNG Simulation. Astrophysical Journal, 2020, 893, 23.	1.6	5
32	The ALMA Spectroscopic Survey Large Program: The Infrared Excess of zÂ=Â1.5–10 UV-selected Galaxies and the Implied High-redshift Star Formation History. Astrophysical Journal, 2020, 902, 112.	1.6	94
33	The mean H <i>α</i> EW and Lyman-continuum photon production efficiency for faint <i>z</i> â‰^ 4â^'5 galaxies. Astronomy and Astrophysics, 2019, 627, A164.	2.1	41
34	Newly Discovered Bright zÂâ^1⁄4Â9–10 Galaxies and Improved Constraints on Their Prevalence Using the Full CANDELS Area. Astrophysical Journal, 2019, 880, 25.	1.6	65
35	Resolved scaling relations and metallicity gradients on sub-kiloparsec scales at z â‰^ 1. Monthly Notices of the Royal Astronomical Society, 2019, 489, 224-240.	1.6	20
36	A Giant Lyα Nebula and a Small-scale Clumpy Outflow in the System of the Exotic Quasar J0952+0114 Unveiled by MUSE ^{â^—} . Astrophysical Journal, 2019, 880, 47.	1.6	15

#	Article	IF	CITATIONS
37	Exploring He†Îl <i>λ</i> 1640 emission line properties at <i>z</i> â^¼2â^'4. Astronomy and Astrophysics, 20 624, A89.	19. 2:1	43
38	The large- and small-scale properties of the intergalactic gas in the Slug Ly α nebula revealed by MUSE He <scp>ii</scp> emission observations. Monthly Notices of the Royal Astronomical Society, 2019, 483, 5188-5204.	1.6	78
39	Probing the ISM of He <scp>ii</scp> λ1640 emitters at <i>z</i> = 2–4 via MUSE. Proceedings of the International Astronomical Union, 2019, 15, 235-239.	0.0	0
40	A Tale of Two Clusters: An Analysis of Gas-phase Metallicity and Nebular Gas Conditions in Proto-cluster Galaxies at zÂâ^1⁄4Â2. Astrophysical Journal, 2019, 883, 153.	1.6	8
41	The MUSE-Wide Survey: survey description and first data release. Astronomy and Astrophysics, 2019, 624, A141.	2.1	76
42	On the lack of correlation between [O <scp>iii</scp>]/[O <scp>ii</scp>] and Lyman continuum escape fraction. Monthly Notices of the Royal Astronomical Society, 2019, 483, 5223-5245.	1.6	40
43	ZFOURGE: Using Composite Spectral Energy Distributions to Characterize Galaxy Populations at 1Â<ÂzÂ<Â4 ^{â^—} . Astrophysical Journal, 2018, 863, 131.	1.6	24
44	Properties and redshift evolution of star-forming galaxies with high [Oâ€III]/[Oâ€II] ratios with MUSE at 0.28Â<Â <i>z</i> Â<Â0.85. Astronomy and Astrophysics, 2018, 618, A40.	2.1	12
45	Near infrared spectroscopy and star-formation histories of 3 ≤i>z ≤ quiescent galaxies. Astronomy and Astrophysics, 2018, 618, A85.	2.1	142
46	The MUSE <i>Hubble</i> Ultra Deep Field Survey. Astronomy and Astrophysics, 2018, 619, A27.	2.1	60
47	Jekyll & Hyde: quiescence and extreme obscuration in a pair of massive galaxies 1.5 Gyr after the Big Bang. Astronomy and Astrophysics, 2018, 611, A22.	2.1	62
48	zfourge: Extreme 5007 Ã Emission May Be a Common Early-lifetime Phase for Star-forming Galaxies at zÂ>Â2.5. Astrophysical Journal, 2018, 869, 141.	1.6	13
49	MUSE Spectroscopic Identifications of Ultra-faint Emission Line Galaxies with M _{UV} Ââ^1⁄4Ââ^15 [*] . Astrophysical Journal Letters, 2018, 865, L1.	3.0	34
50	Nearly all the sky is covered by Lyman-α emission around high-redshift galaxies. Nature, 2018, 562, 229-232.	13.7	108
51	First Data Release of the COSMOS Lyα Mapping and Tomography Observations: 3D Lyα Forest Tomography at 2.05Â<ÂzÂ<Â2.55. Astrophysical Journal, Supplement Series, 2018, 237, 31.	3.0	80
52	ZFIRE: 3D Modeling of Rotation, Dispersion, and Angular Momentum of Star-forming Galaxies at z â^¼ 2. Astrophysical Journal, 2018, 858, 47.	1.6	16
53	First gas-phase metallicity gradients of 0.1 ≲ z ≲ 0.8 galaxies with MUSE. Monthly Notices of the Royal Astronomical Society, 2018, 478, 4293-4316.	1.6	47
54	Decoupled black hole accretion and quenching: the relationship between BHAR, SFR and quenching in Milky Way- and Andromeda-mass progenitors since zÂ=Â2.5. Monthly Notices of the Royal Astronomical Society, 2018, 473, 3710-3716.	1.6	4

#	Article	IF	CITATIONS
55	ZFIRE: The Evolution of the Stellar Mass Tully–Fisher Relation to Redshift â^¼2.2. Astrophysical Journal, 2017, 839, 57.	1.6	26
56	A massive, quiescent galaxy at a redshift of 3.717. Nature, 2017, 544, 71-74.	13.7	167
57	Discovery of Extreme [O iii]+Hβ Emitting Galaxies Tracing an Overdensity at z â^1⁄4 3.5 in CDF-South ^{â^—} . Astrophysical Journal Letters, 2017, 838, L12.	3.0	32
58	The Size Evolution of Star-forming Galaxies since zÂâ^1⁄4Â7 Using ZFOURGE. Astrophysical Journal Letters, 2017, 834, L11.	3.0	57
59	ZFIRE: SIMILAR STELLAR GROWTH IN Hα-EMITTING CLUSTER AND FIELD GALAXIES AT z â^¼ 2. Astrophysical Journal, 2017, 834, 101.	1.6	14
60	ZFIRE: using Hα equivalent widths to investigate the in situ initial mass function at zÂâ^¼Â2. Monthly Notices of the Royal Astronomical Society, 2017, 468, 3071-3108.	1.6	19
61	Effect of Local Environment and Stellar Mass on Galaxy Quenching and Morphology at 0.5 < z < 2.0 [*] . Astrophysical Journal, 2017, 847, 134.	1.6	106
62	ZFIRE: A KECK/MOSFIRE SPECTROSCOPIC SURVEY OF GALAXIES IN RICH ENVIRONMENTS AT z $\hat{a}^{1}/_{4}$ 2. Astrophysical Journal, 2016, 828, 21.	1.6	53
63	DIFFERENCES IN THE STRUCTURAL PROPERTIES AND STAR FORMATION RATES OF FIELD AND CLUSTER GALAXIES AT Z â^¼ 1. Astrophysical Journal, 2016, 826, 60.	1.6	17
64	SATELLITE QUENCHING AND GALACTIC CONFORMITY AT 0.3 < z < 2.5*. Astrophysical Journal, 2016, 817, 9.	1.6	50
65	THE SFR–M _* RELATION AND EMPIRICAL STAR FORMATION HISTORIES FROM ZFOURGE AT 0.5 < z < 4*. Astrophysical Journal, 2016, 817, 118.	1.6	241
66	ZFIRE: THE KINEMATICS OF STAR-FORMING GALAXIES AS A FUNCTION OF ENVIRONMENT AT z â^1/4 2. Astrophysical Journal Letters, 2016, 825, L2.	3.0	14
67	LARGE-SCALE STRUCTURE AROUND A $z = 2.1$ CLUSTER. Astrophysical Journal, 2016, 826, 130.	1.6	38
68	THE FOURSTAR GALAXY EVOLUTION SURVEY (ZFOURGE): ULTRAVIOLET TO FAR-INFRARED CATALOGS, MEDIUM-BANDWIDTH PHOTOMETRIC REDSHIFTS WITH IMPROVED ACCURACY, STELLAR MASSES, AND CONFIRMATION OF QUIESCENT GALAXIES TO zÂâ^1⁄4Â3.5*. Astrophysical Journal, 2016, 830, 51.	1.6	166
69	Radio galaxies in ZFOURGE/NMBS: no difference in the properties of massive galaxies with and without radio-AGN out to <i>z</i> Â=Â2.25. Monthly Notices of the Royal Astronomical Society, 2016, 455, 2731-2744.	1.6	22
70	UV TO IR LUMINOSITIES AND DUST ATTENUATION DETERMINED FROM â^1⁄44000 K-SELECTED GALAXIES AT 1 < < 3 IN THE ZFOURGE SURVEY*. Astrophysical Journal Letters, 2016, 818, L26.	^Z 3.0	27
71	ZFOURGE catalogue of AGN candidates: an enhancement of 160-μm-derived star formation rates in active galaxies to <i>z</i> Â=Â3.2. Monthly Notices of the Royal Astronomical Society, 2016, 457, 629-641.	1.6	45
72	Z-FIRE: ISM PROPERTIES OF THE <i>z</i> = 2.095 COSMOS CLUSTER. Astrophysical Journal, 2016, 819, 100.	1.6	25

Themiya Nanayakkara

#	Article	IF	CITATIONS
73	COLD-MODE ACCRETION: DRIVING THE FUNDAMENTAL MASS–METALLICITY RELATION AT zÂâ^¼Â2. Astrophy Journal Letters, 2016, 826, L11.	sical 3.0	45
74	THE ABSENCE OF AN ENVIRONMENTAL DEPENDENCE IN THE MASS–METALLICITY RELATION AT <i>z</i> = 2. Astrophysical Journal Letters, 2015, 802, L26.	3.0	58
75	THE SIZES OF MASSIVE QUIESCENT AND STAR-FORMING GALAXIES AT <i>z</i> â^¼ 4 WITH ZFOURGE AND CANDELS. Astrophysical Journal Letters, 2015, 808, L29.	3.0	64
76	ZFIRE: GALAXY CLUSTER KINEMATICS, H <i>α</i> STAR FORMATION RATES, AND GAS PHASE METALLICITIES OF XMM-LSS J02182-05102 AT \${z}_{mathrm{cl}}=1.6233\$. Astrophysical Journal, 2015, 811, 28.	1.6	54
77	Can we infer the Initial Mass Function of galaxies at z ~ 2?. Proceedings of the International Astronomical Union, 2015, 11, 35-38.	0.0	0
78	ZFOURGE/CANDELS: ON THE EVOLUTION OF <i>M</i> * GALAXY PROGENITORS FROM <i>z</i> = 3 TO 0.5. Astrophysical Journal, 2015, 803, 26.	1.6	104
79	THE DIFFERENTIAL SIZE GROWTH OF FIELD AND CLUSTER GALAXIES AT <i>z</i> = 2.1 USING THE ZFOURGE SURVEY. Astrophysical Journal, 2015, 806, 3.	1.6	31
80	KECK/MOSFIRE SPECTROSCOPIC CONFIRMATION OF A VIRGO-LIKE CLUSTER ANCESTOR AT <i>z</i> = 2.095. Astrophysical Journal Letters, 2014, 795, L20.	3.0	63
81	THE DISTRIBUTION OF SATELLITES AROUND MASSIVE GALAXIES AT 1 < <i>z</i> < 3 IN ZFOURGE/CANDELS: DEPENDENCE ON STAR FORMATION ACTIVITY. Astrophysical Journal, 2014, 792, 103.	1.6	24
82	EXPLORING THE <i>z</i> = 3-4 MASSIVE GALAXY POPULATION WITH ZFOURGE: THE PREVALENCE OF DUSTY AND QUIESCENT GALAXIES. Astrophysical Journal Letters, 2014, 787, L36.	3.0	80